Available online at www.sciencedirect.com
SCIENCE DIRECT
Talanta 68 (2006) 629–635
Talanta
www.elsevier.com/locate/talanta

Direct detection of trimethylamine in meat food products using ion mobility spectrometry

Gheorghe M. Bota, Peter B. Harrington *

Ohio University, Center for Intelligent Chemical Instrumentation, Department of Chemistry and Biochemistry, Clippinger Laboratories, Athens, OH 45701-2979, USA

Received 4 November 2004; received in revised form 3 May 2005; accepted 4 May 2005
Available online 23 June 2005

Abstract

Biogenic amines are degradation products generated by bacteria in meat products. These amines can indicate bacterial contamination or have a carcinogenic effect to humans consuming spoiled meats; therefore, their rapid detection is essential. Trimethylamine (TMA) is a good target for the detection of biogenic amines because its volatility. TMA was directly detected in meat food products using ion mobility spectrometry (IMS). TMA concentrations were measured in chicken meat juice for a quantitative evaluation of the meat decaying process. The lowest detected TMA concentration in chicken juice was 0.6 ± 0.2 ng and the lowest detected signal for TMA in a standard aqueous solution was 0.6 ng. IMS data were processed using partial least squares (PLS) and Fuzzy rule-building expert system (FuRES). Using these two chemometric methods, trimethylamine concentrations of different days of meat spoilage can be separated, indicating the decaying of meat products. Comparing the two methods, FuRES provided a better classification of different days of meat spoilage.

Keywords: Ion mobility spectrometry (IMS); Biogenic amines; Trimethylamine (TMA); Meat food products; Meat spoilage; Partial least squares (PLS); Fuzzy rule-building expert system (FuRES); Chemometrics

1. Introduction

The quality of meat food products can be evaluated by the presence of some volatile or semi-volatile compounds such as the biogenic amines. Biogenic amines are simple nitrogen compounds derived from amino acids in which one or all hydrogen atoms are substituted by various alkyl or aryl radicals. Biogenic amines are formed by the activity of bacterial amino acid decarboxylases during the degradation processes of proteins. Some biogenic amines have names derived from corresponding amino acids; for example, histamine from histidine, tyramine from tyrosine, and tryptamine from tryptophan. Other biogenic amines have specific names such as trimethylamine (TMA), dimethylamine, cadaverine, and putresceine [1,2]. In the human body, biogenic amines play important physiological roles, such as in the formation and maintenance of synapses and in the generation of endogenous amino acids [3].

Different types of food and beverage contain various biogenic amines that are formed during food processing or storage and can indicate the degree of spoilage by microbial activity. Biogenic amines have been detected and measured in fish [4–9], meat [10–14], sausages [15–17], milk [18], cheese [19], vegetable products [20], wine [21], and beer [22]. Biogenic amines in food are metabolized by enzymatic reactions in the human body to harmless final products. Diamine oxidase (DAO) detoxifies amines in the human intestine while monoamine oxidase (MAO) performs the same function in different tissues of the human body. Both enzyme activities can be diminished or suppressed due to genetic predisposition, gastrointestinal diseases, or by certain inhibitors like medicines or alcohol. In such cases, biogenic amines are introduced into the blood stream and at high enough concentrations may be toxic. Biogenic amines are precursors of carcinogenic N-nitroso compounds. Lower concentrations of

* Corresponding author. Tel.: +1 740 517 8458; fax: +1 740 593 0148.
E-mail address: peter.harrington@ohio.edu (P.B. Harrington).

0039-9140/$ – see front matter © 2005 Elsevier B.V. All rights reserved.
doi:10.1016/j.talanta.2005.05.001

biogenic amines in the blood stream may cause hypotension through dilatation of peripheral blood vessels, headaches, nausea, respiratory distress, abdominal cramps, and vomiting. Therefore, the concentration of biogenic amines in foods has to be evaluated so that the safe levels are maintained. An increase in concentration of biogenic amines indicates food spoilage, representing a threat to food safety. The most widely detected biogenic amine is trimethylamine due to its fishy-odor, and it has been used as an indicator of fish spoilage [8]. TMA is encountered in other food products as well [8].

Different tests and methods (organoleptic, total volatile basic nitrogen index, TVB-N) have been used to detect biogenic amines in food that correlate with spoilage [5]. Organoleptic tests are limited by their very high detection limits therefore, other analytical methods are used such as high performance liquid chromatography (HPLC) [13,23], gas chromatography-flame ionization detection (GC-FID) [24], gas chromatography-mass spectrometry (GC–MS) [25], and capillary electrophoresis (CE) [26,27]. More recent analytical methods used for biogenic amine detection are amperometric bi-enzyme electrodes [6], metalloporphyrins-coated quartz microbalance sensor array (electronic nose) [7,18], and ion mobility spectrometry (IMS) [10].

Each of these analytical detection methods presents advantages and disadvantages. Total volatile basic nitrogen index determines the total amounts of amines but gives no indication about the types of amines present. Chromatographic methods require extra sample preparation (derivatization) to reduce or eliminate column memory effects. Ion mobility spectrometry is simple, fast, highly selective, and very sensitive to a wide range of compounds making it very attractive as a detection method for biogenic amines.

IMS characterizes chemical compounds through their ion gas-phase mobilities in a weak electric field. Compounds with different mobilities will have different drift times in a spectrum and in this way they can be detected. IMS is an important analytical tool for identification of chemical warfare agents [28], pesticides [29], and bacterial products [30]. The ion mobility coefficient can be obtained using the drift velocity of ions in an electric field of 100 V/cm. The expression for the drift velocity v_d is given in

$$v_d = KE \tag{1}$$

for which K is the ion mobility coefficient and E the electric field. The ions move through a counter-current of drift gas under the influence of an electric field. Amines are easily studied by IMS due to their high proton affinity. In IMS, protonated monomer, dimer, fragment ions, and complex oligomeric ions may be formed [31,32].

For constant temperature, pressure, electric field intensity, and length of drift region, reduced mobilities can be determined according to the formula:

$$K_{0(\mathrm{unk})} = \frac{K_{0(\mathrm{cal})} t_{(\mathrm{cal})}}{t_{(\mathrm{unk})}} \tag{2}$$

for which $K_{0(\mathrm{unk})}$ is the ion reduced mobility for the unknown, $K_{0(\mathrm{cal})}$ is the ion reduced mobility for the calibrant, $t_{(\mathrm{cal})}$ is drift time of the calibrant and $t_{(\mathrm{unk})}$ is the drift time of unknown. Nicotinamide was used as the calibrant in these studies, with ion mobility value of 1.85 $\mathrm{cm^2\ V^{-1}\ s^{-1}}$ [31].

Spectra for the biogenic amines were collected with a Barringer IONSCAN 350 spectrometer in positive ion mode. Trimethylamine ions were obtained by a charge transfer reaction from the nicotinamide reagent ion used by this spectrometer.

For data processing three different chemometric methods were used: fuzzy rule-building expert system (FuRES) [33], partial least squares (PLS) [35,36], and principal component analysis (PCA) [34,37].

PCA is a multivariate chemometric technique that is used to display relationships among the different spectra [34,37]. The spectra comprise the rows and the drift time measurements comprise the columns of data matrix **D**. PCA decomposes the matrix **D** into two smaller matrices **T** and **P** as given in Eq. (4).

$$\mathbf{D} = \mathbf{T} \cdot \mathbf{P} + \mathbf{E} \tag{4}$$

Matrix **T** comprises spectral scores as columns for each principal component. Matrix **P** comprises the variable loadings for which each component is a row vector. The number of columns of **T** and rows of **P** is the number of principal components. **E** is the residual matrix. An eigenvalue of the principal component obtained as the sum of squares of each score vector (i.e., column of **T**) characterizes the relative importance of each principal component. Usually eigenvalues of principal components are represented as percentages of the entire dataset to give the percent cumulative variance. The principal component scores will be used to visualize the overall relations among the spectra in the data.

PLS is related to PCA, except a common set of components are found between matrices of dependent and independent variables [34,35]. The data matrix **D** comprises the independent variables and is decomposed as in Eq. (4) in **T**, the score matrix and **P**, the loading matrix. Matrix **A**, that comprises the dependent variables, is decomposed into a matrix of scores **U**, and loadings **Q**, and **F** is a matrix that comprises residual errors of the dependent variables in Eq. (5).

$$\mathbf{A} = \mathbf{U} \cdot \mathbf{Q} + \mathbf{F} \tag{5}$$

The PLS algorithm maximizes the covariance between **T** and **U**. The scores **U** can be computed using the scores **T** and the regression coefficients matrix **B** in Eq. (6).

$$\mathbf{U} = \mathbf{T} \cdot \mathbf{B} \tag{6}$$

The regression coefficients matrix **B** is calculated according to Eq. (7)

$$\mathbf{B} = (\mathbf{T}^{\mathrm{T}} \cdot \mathbf{T})^{-1} (\mathbf{T}^{\mathrm{T}} \cdot \mathbf{U}) \tag{7}$$

In this way dependent variables **A** can be predicted from independent variables **D** using the PLS regression model.

A fuzzy rule-building expert system is an expert system used for spectra classification [33]. In FuRES, a classification tree is built that is comprised of branches of temperature constrained sigmoidal logistic functions. The logistic functions minimize the classification entropy. The computational temperature is optimized so that the first derivative of the classification entropy is maximized. The logistic functions are optimal with respect to fuzziness. The output of the FuRES tree will be a series of fuzzy membership functions that sum to unity for each object.

2. Experimental

2.1. Instrumentation

The ion mobility spectrometer used in this work was a Barringer IONSCAN 350 (Barringer Instruments Inc., New Providence, NJ). A schematic representation of the ion mobility spectrometer is adapted from [38] in Fig. 1. The spectra were acquired in positive ion mode and the instrument was set for narcotics detection. The data acquisition frequency was 80 kHz and every spectrum had 1600 data points. The acquisition data board was a National Instruments AT-MIO-16XE-10 board connected to a Pentium Pro 200 Mhz computer. A home-built LabVIEW® 5.1 virtual instrument was used for data acquisition. The shutter grid width was 200 μs and spectra were collected with a scan period of 25 ms. The internal calibrant was nicotinamide with a reduced mobility of 1.85 $cm^2\ V^{-1}\ s^{-1}$. The following flow parameters were established: drift flow was 200 $cm^3\ min^{-1}$, sample flow 200 $cm^3\ min^{-1}$, and resultant exhaust flow was 400 $cm^3\ min^{-1}$. The temperatures for the inlet and drift tube were 294 and 233 °C, respectively and were kept constant during the experiment. The sample desorption heater was set to 300 °C. The desorber was activated when the sample was inserted and the sample held in the heated zone for 20 s.

2.2. Materials

Standard solutions were made of trimethylamine hydrochloride (Sigma, St. Louis, MO, 98% analytical purity) taken directly from the container. Concentrations were: 0.2 ppm (0.2 $\mu g\ mL^{-1}$), 0.3 ppm (0.3 $\mu g\ mL^{-1}$), 0.4 ppm (0.4 $\mu g\ mL^{-1}$), 0.5 ppm (0.5 $\mu g\ mL^{-1}$), 1 ppm (1 $\mu g\ mL^{-1}$), 3 ppm (3 $\mu g\ mL^{-1}$), and 5 ppm (5 $\mu g\ mL^{-1}$). Each standard solution was prepared using class A glassware by dissolving TMA hydrochloride in 1000.0 mL of deionized water. All standard solution concentrations were corrected for 98% analytical purity. Solutions were homogenized for 2 h on a stirring plate using a magnetic stirrer.

The juice from spoiled meat was collected using glass fiber filter disks (Fisher Scientific, Pittsburgh, PA; diameter 4.25 cm). The blank glass fiber filter disks were sampled in the

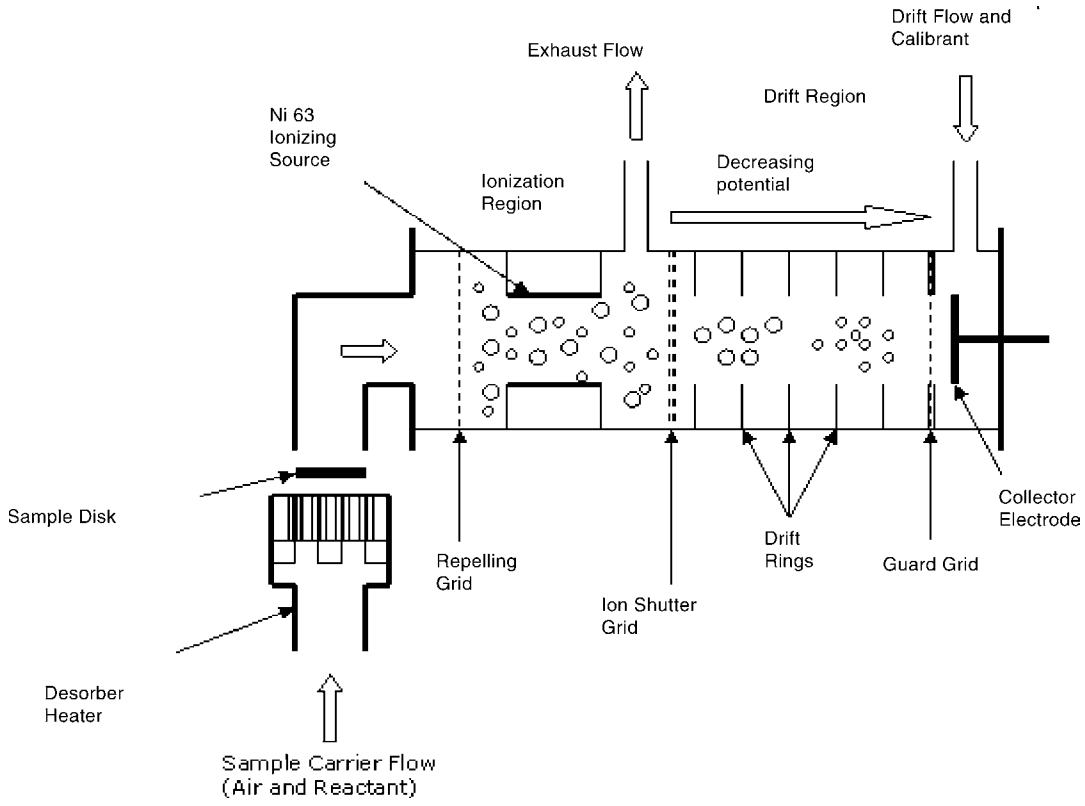

Fig. 1. Schematic representation of Barringer IONSCAN 350 adapted from [38].

thermal desorber unit of the IONSCAN until no background signal was observed from any volatile contaminants before use.

The chicken meat was dated by the labeling on package that gave the day it was made available for sale. The liquid from the container holding the chicken meat was collected for the experiment. The liquid from the container was water-based and represented a noninvasive sample of the chicken meat. This liquid is hence referred to as chicken juice. The pH of the chicken juice was determined to be 5.8.

Chicken juice in 10 mL aliquots was delivered to sterile polystyrene test tubes 16 mm × 125 mm, with screw cap lids (Fisher Scientific, Pittsburgh, PA). The test tubes with juice were centrifuged for 10 min at 4000 rpm with a centrifuge. After centrifuging the chicken juice only the clear part of the liquid was decanted and used for the experiments.

Samples of TMA solutions and meat juice were collected with a 10-μL Hamilton syringe (Hamilton Company, Reno, NV). TMA solutions of 5 μL were spotted on the fiber glass sample disk that was inserted into the ion mobility spectrometer thermal desorber. Only 1 μL of chicken meat juice was spotted on the sampling disk because the main goal was to detect the lowest TMA concentration in the sample juice.

For the chicken juice, two sets of data were collected. The juice was stored in a refrigerator at 6.0 °C and 2-mL aliquots of juice were removed, put in glass vials that were closed with screw caps and allowed to decompose at room temperature. Each juice vial was aged for a different number of days during a five days period. The first vial was aged for 5 days, the second for 4 days, the third for 3 days, the fourth for 2 days and the fifth was aged for 1 day. On the sixth day the spectra were collected for each vial. A random block design was used with five replicates for collecting spectra. This data set was used for model building.

The second data set was used for validation. Aliquots of 5 mL juice were placed in a glass vial closed with a screw cap and allowed to decompose at room temperature. For a 5-day period, spectra of chicken juice were collected daily from the vial in the hood, and analyzed using a 1 μL aliquot applied to the sampling disk, same sample volume as in the previous method.

3. Data processing

Several hundred spectra were acquired for each measurement. The model-building data set comprised 18 IMS measurements of chicken juice. The validation data set comprised 15 IMS measurements. The measurement sets of spectra were preprocessed and then the five spectra with the largest TMA peak intensities were extracted. The first preprocessing step eliminated drift time measurements less than 0.5 ms, to remove the gating pulse from the spectra. Each spectrum comprised 1560 data points after removal of the gating pulse. Each spectrum was baseline corrected by subtracting the average of the intensities of the spectra calculated from the range of [0.5, 6] ms from every point in the spectrum. Because charge is conserved in IMS, each spectrum was normalized to unit area. After selecting five spectra from each measurement set, the model building set comprised 90 spectra and the validation set comprised 75 spectra.

All data sets were mean-centered before PCA analysis. The first PC correlates well with the age of the chicken juice. Discriminant PLS was used to build a classification model [39]. Two binary target matrices **A** were used. The first grouped the spectra into good, fair, and bad, and the second grouped the spectra into good and bad classes.

Cross-validation of the training set was used to optimize the PLS model. Cross-validation removed each measurement as opposed to spectrum so all five replicate spectra were removed for each cross-validation step. The validation data set was used for prediction. The largest estimate $\hat{\mathbf{a}}_i$ designated the class of spectrum *i*. FuRES has an advantage over other supervised classification methods in that it does not have to configure any parameters during model building, such as the number of latent variables in PLS and training cycles with artificial neural networks. The classification tree was built and evaluated using the same matrices as those used for PLS. The same criterion as for the PLS models for class designation was used, the maximum estimate.

4. Results and discussion

The reduced mobility calculated for TMA was 2.36 $cm^2\ V^{-1}\ s^{-1}$ and corresponded to a value reported in the literature [31]. The scores on the first two principal components of the model-building data set and the validation set are given in Figs. 2 and 3, respectively. The first principal component spans the age of the samples. After the second day, the TMA peak was large enough to saturate the instrument so although there is some separation of days 2–4,

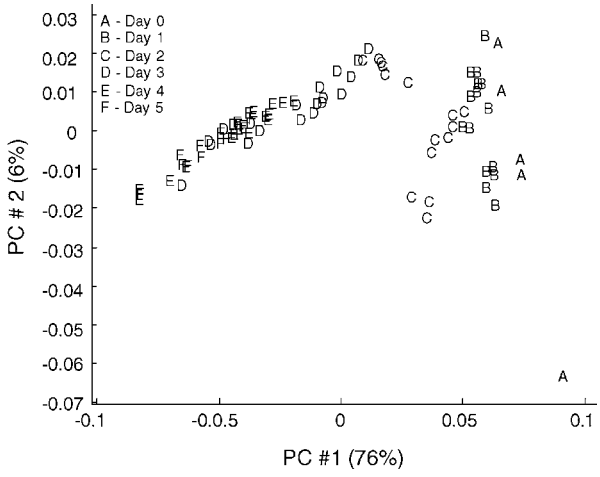

Fig. 2. Principal component scores for the model-building data set of positive ion mobility spectra of aged chicken juice. Numbers in parenthesis represent the percentage of principal components in the data set.

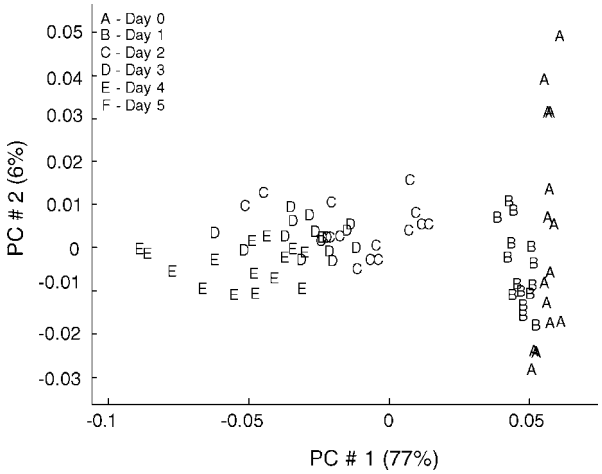

Fig. 3. Principal component scores for the validation set of positive ion mobility spectra of aged chicken juice. Numbers in parenthesis represent the percentage of principal components in the data set.

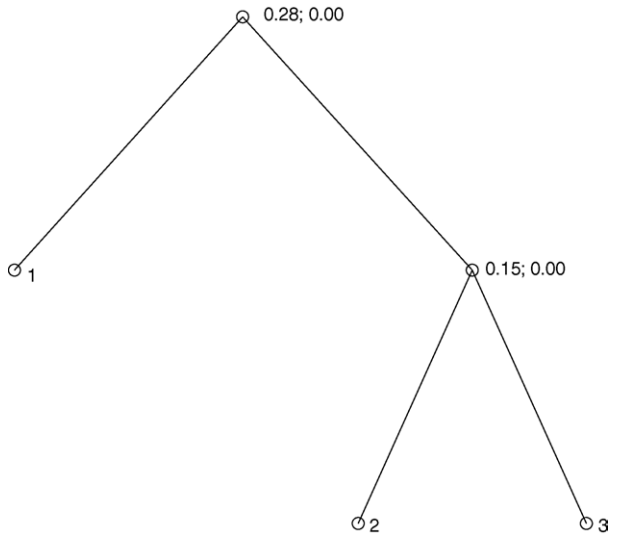

Fig. 4. FuRES classification tree for fresh (1), fair (2), and bad (3) classes.

the spectral scores were overlapping. Therefore, different grades of meat spoilage were grouped into fresh, fair, and bad. The model-building and validation data sets are very similar even though they were collected 6 days apart.

Using cross-validation by measurement and not replicate, the optimum number of latent variables was 9 for the three class matrix. The PLS results for the validation data are presented in a confusion matrix given in Table 1(a). The confusion matrix for the three classes gives the actual class as rows and estimated class by column. A similar confusion matrix was generated for FuRES classification. The FuRES confusion matrix is given in Table 1(b). FuRES classification tree for three classes (fresh, fair, and bad) is given in Fig. 4. These results suggested that the good and fair classes were confused by both methods, although the FuRES method was superior to PLS.

The fair and bad classes were combined into one class, and the PLS and FuRES models were built for the two class binary target matrix. The optimum number of latent variables in the PLS model was 8 using the same cross-validation procedure.

Besides FuRES, a univariate classification model was also used as a control that processed the TMA peak intensity. This method was the same that would be used in a classical peak-window based algorithm. Two criteria were evaluated. The first method classified any spectrum with a TMA peak intensity larger than the maximum peak intensity in the spectra from the fresh class of the training set as bad. The second criterion classified any spectrum below the minimum peak intensity in the spectra from the bad class of the training set as good. The reason two criteria were evaluated was that the TMA peak intensities were overlapping among the spectra in the training set that corresponded to the fresh and bad quality classes.

For the two class models, the results are reported in Tables 2 and 3. as confusion matrices. The PLS model failed

Table 1
Confusion matrices for classification by IMS in three classes: fresh, fair, and bad

	Fresh	Fair	Bad
(a) Confusion matrix generated using the predicted errors in PLS method			
Fresh	1	13	1
Fair	0	15	0
Bad	0	45	0
(b) Confusion matrix generated using the predicted errors in FuRES method			
Fresh	10	5	0
Fair	0	15	0
Bad	0	0	45

Table 2
Confusion matrices for prediction of IMS spectra of chicken juice in two classes: fresh and bad

	Fresh	Bad
(a) Confusion matrix generated using the predicted errors in PLS method		
Fresh	0	15
Bad	0	60
(b) Confusion matrix generated using the predicted errors in FuRES method		
Fresh	13	2
Bad	0	60

Table 3
Confusion matrices for prediction of IMS spectra of chicken juice in two classes: fresh and bad using the TMA peak height

	Fresh	Bad
(a) Using the intensity threshold of the largest TMA peak from the spectra of the good class		
Fresh	11	4
Bad	2	58
(b) Using the intensity threshold of the lowest TMA peak from the spectra of the bad class		
Fresh	10	5
Bad	1	59

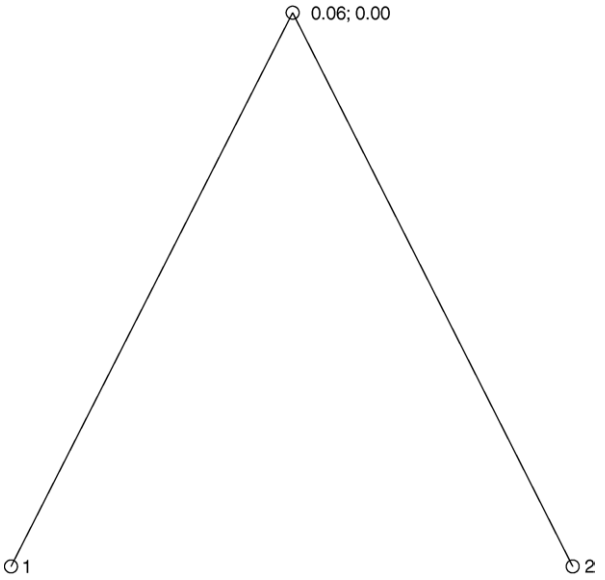

Fig. 5. FuRES classification tree for fresh (1) and bad (2) classes.

for the validation data set. This failure may have resulted from overfitting of the PLS model by the cross validation procedure, but the PLS results were in general poor for the validation set regardless of the number of latent variables used in the model.

The FuRES classification tree for two classes (fresh and bad) is given in Fig. 5. The control results of using univariate TMA peak heights are given in Table 3. In this case, the peak window technique worked better than the PLS model, but not as well as FuRES. The reason is that FuRES also takes advantage of other peaks that may appear in the spectra besides TMA. These additional peaks could be other microbial products or oligomeric TMA ions.

Trimethylamine content in meat juice was evaluated quantitatively using a random block design. The detection limit of the ion mobility spectrometer was determined using a calibration line of standard TMA solutions in water. For each standard, three replicates were analyzed in a random block design. The ion mobility spectra acquired from fresh chicken juice and a 1 μL of a 3 ppm TMA solution is given in Figs. 6 and 7, respectively.

For each measurement, the TMA concentration profile was used to select a set that comprised between 50 and 100 spectra to be averaged. Therefore, each measurement furnished a single average spectrum for which the TMA peak was the largest and stable. The peak intensity of TMA from this average spectrum was used for calibration. The calibration line with 95% confidence interval was used to define the limit of detection. The detection limit was the concentration where the lower limit equals the upper limit at the ordinate. The limit of detection within this interval was 0.6 ng. The sensitivity was $1.12 \pm 0.15\ \mathrm{V\,ng^{-1}}$ with a 95% confidence interval. Fig. 8 gives the TMA calibration line.

The TMA concentration in chicken juice was calculated using standard addition with 10 μL of the aqueous stan-

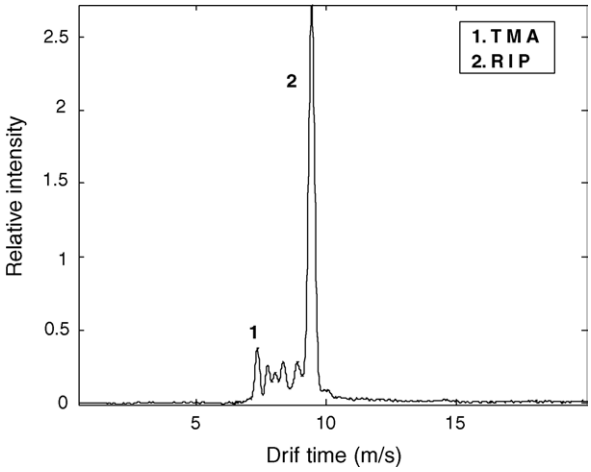

Fig. 6. IMS spectrum of TMA in fresh chicken juice. Reaction ion peak (RIP) is nicotinamide.

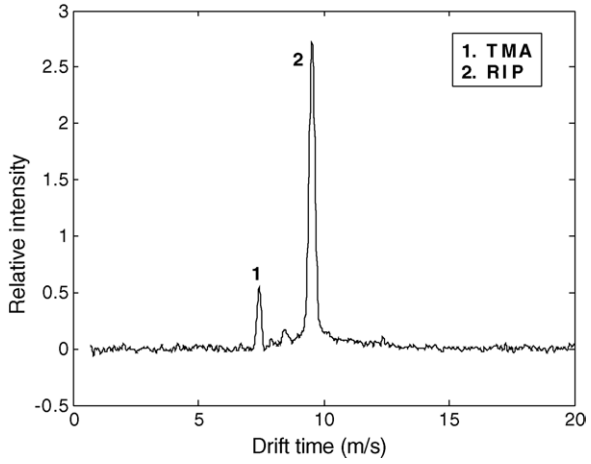

Fig. 7. IMS spectrum of 3 ppm TMA solution. Reaction ion peak (RIP) is nicotinamide.

dard TMA solutions added to 990 μL of chicken juice. For every sample, three replicates were obtained and TMA peak intensity was evaluated using the same procedure as for the TMA calibration line. Using the standard addition method, the TMA mass was 0.6 ± 0.2 ng and corresponded a to 0.6 ± 0.2 ppm TMA concentration in chicken juice. Fig. 9

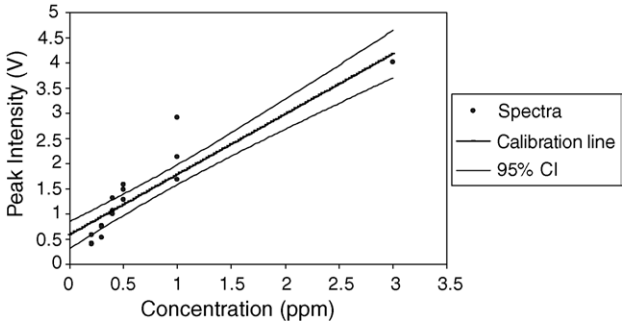

Fig. 8. Calibration line generated for pure TMA solutions in order to determine the lowest detection limit for TMA.

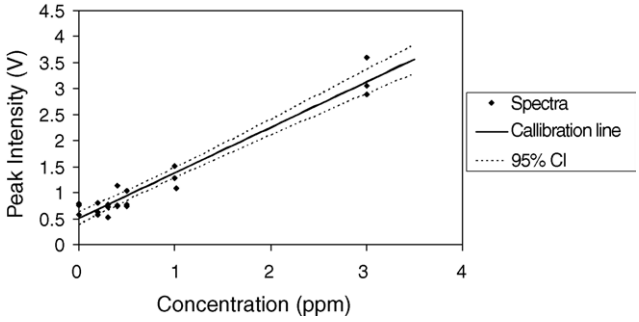

Fig. 9. Calibration line generated for standard addition method. Standard TMA solutions were added to meat juice in order to evaluate quantitatively initial TMA concentration in juice.

gives the calibration line for TMA concentration in chicken juice.

5. Conclusions

This work demonstrated that trimethylamine in chicken juice (i.e., external liquid) can be detected directly and quantitatively evaluated using ion mobility spectrometry. The lowest detected TMA concentration in chicken juice was 0.6 ± 0.2 ng and the lowest detection limit for TMA standard solutions was 0.3 ± 0.2 ng. The method proved to be very sensitive and the results were reproducible. The sensitivity for TMA in water was $1.12 \pm 0.15\ \mathrm{V\,ng^{-1}}$ with a 95% confidence interval. Meat juice offers a better alternative than the raw meat for biogenic amines detection.

Although IMS is most often used as a qualitative technique, quantitative results can be obtained too. IMS may provide a rapid screening method for meat quality using juice. Chemometric methods used for processing the IMS data allowed a classification of different spoilage grades for meat juice. PLS classification of fresh and bad samples was not able to distinguish between the two classes. Compared to PLS, FuRES had only two misclassified spectra for the fresh and bad evaluation. FuRES also performed better than the classic IMS approach of using the single TMA peak occurs in a drift time window, because FuRES uses all the peaks in the spectra for classification. All these results demonstrate the robustness of the FuRES method.

Acknowledgements

The Center for Intelligent Chemical Instrumentation and U.S. Air Force is thanked for their support of this research. The Federal Aviation Administration is thanked for the loan of the Barringer IONSCAN 350. The Research Corporation is acknowledged for the research opportunity award. The authors would like to thank Klaus Himmeldirk, Preshious Rearden, Mariela Ochoa, Matt Rainsberg, Ping Chen, and Cynthia Medford for their help, comments and suggestions.

References

[1] M.H.S. Santos, Int. J. Food Microbiol. 29 (1996) 213–231.
[2] S. Bodmer, M. Kneubuhl, C. Imark, Inflamm. Res. 48 (1999) 296–300.
[3] N. Okado, M. Narita, N. Narita, Brain Dev. (2001) S11–S15.
[4] R. Stute, K. Petridis, H. Steinhart, G. Biernoth, Eur. Food Res. Technol. 215 (2002) 101–107.
[5] C. Ruiz-Capillas, A. Moral, Food Res. Int. 34 (2001) 441–447.
[6] M. Niculescu, C. Nistor, I. Frebort, P. Pec, B. Mattiasson, E. Csoregi, Anal. Chem. 72 (2000) 1591–1597.
[7] C. diNatale, J.A.J. Brunink, F. Bungaro, F. Davide, A. dAmico, R. Paolesse, T. Boschi, M. Faccio, G. Ferri, Meas. Sci. Technol. 7 (1996) 1103–1114.
[8] S. Sadok, R.F. Uglow, S.J. Haswell, Anal. Chim. Acta 321 (1996) 69–74.
[9] A. Bene, A. Hayman, E. Reynard, J.L. Luisier, J.C. Villettaz, Sens. Actuator B, Chem. 72 (2001) 204–207.
[10] Z. Karpas, B. Tilman, R. Gdalevsky, A. Lorber, Anal. Chim. Acta 463 (2002) 155–163.
[11] C.M.G. Silva, M.B.A. Gloria, Food Chem. 78 (2002) 241–248.
[12] A.M. Nassar, W.H. Emam, Nahr. Food 46 (2002) 197–199.
[13] I. Kaniou, G. Samouris, T. Mouratidou, A. Eleftheriadou, N. Zantopoulos, Food Chem. 74 (2001) 515–519.
[14] G. Vinci, M.L. Antonelli, Food Control 13 (2002) 519–524.
[15] J.D. Coisson, C. Cerutti, F. Travaglia, M. Arlorio, Meat Sci. 67 (2004) 343–349.
[16] C. Ruiz-Capillas, F. Jimenez-Colmenero, Eur. Food Res. Technol. 218 (2004) 237–241.
[17] E. Parente, M. Martuscelli, F. Gardini, S. Grieco, M.A. Crudele, G. Suzzi, J. Appl. Microbiol. 90 (2001) 882–891.
[18] S. Ampuero, T. Zesiger, V. Gustafsson, A. Lunden, J.O. Bosset, Eur. Food Res. Technol. 214 (2002) 163–167.
[19] S. Vale, M.B.A. Gloria, Food Chem. 63 (1998) 343–348.
[20] P. Kalac, S. Svecova, T. Pelikanova, Food Chem. 77 (2002) 349–351.
[21] A. Lonvaud-Funel, FEMS Microbiol. Lett. 199 (2001) 9–13.
[22] A. Slomkowska, W. Ambroziak, Eur. Food Res. Technol. 215 (2002) 380–383.
[23] M.R. Alberto, M.E. Arena, M.C.M. de Nadra, Food Control 13 (2002) 125–129.
[24] Y.C. Chien, S.N. Uang, C.T. Kuo, T.S. Shih, J.F. Jen, Anal. Chim. Acta 419 (2000) 73–79.
[25] G.A. Mills, V. Walker, H. Mughal, J. Chromatogr. B 723 (1999) 281–285.
[26] N.P. Beard, A.J. de Mello, Electrophoresis 23 (2002) 1722–1730.
[27] M. Timm, B.M. Jorgensen, Food Chem. 76 (2002) 509–518.
[28] G.R. Asbury, C. Wu, W.F. Siems, H.H. Hill, Anal. Chim. Acta 404 (2000) 273–283.
[29] K. Tuovinen, H. Paakkanen, O. Hanninen, Anal. Chim. Acta 404 (2000) 7–17.
[30] N.J.C. Strachan, F.J. Nicholson, I.D. Ogden, Anal. Chim. Acta 313 (1995) 63–67.
[31] Z. Karpas, Anal. Chem. 61 (1989) 684–689.
[32] G.A. Eiceman, Z. Karpas (Ed.), Ion Mobility Spectrometry, CRC Press, Boca Raton, 1994, pp. 34–37.
[33] P.D. Harrington, J. Chemometr. 5 (1991) 467–486.
[34] H. Wold, in: P.R. Krishnaiah (Ed.), Multivariate Analysis, Academic Press, New York, 1966, pp. 391–420.
[35] H. Wold, in: J. Gani (Ed.), Perspectives in Probability and Statistics, Academic Press, London, 1975.
[36] H. Hotelling, J. Educ. Psy. 24 (1933) 417–441.
[37] E.R. Malinowski, Factor Analysis in Chemistry, second ed., John Wiley & Sons, Inc., New York, 1991.
[38] Barringer Instruments Ionscan Model 350 Operator's Manual, New Providince, NJ, 1993.
[39] E.K. Kemsley, Chemometr. Intell. Lab. Syst. 33 (1996) 47–61.